Design and Analysis of 4-DOF Cable-Driven Parallel Mechanism

Darwin Lau, Trevor Hawke, Louis Kempton, Denny Oetomo, Saman Halgamuge
University of Melbourne, Australia
dtlau@pgrad.unimelb.edu.au, {doetomo, saman}@unimelb.edu.au

Abstract

The design and analysis of a 4-DOF multi-link cable driven parallel mechanism is presented. In contrast to many existing cable driven parallel mechanism, the proposed manipulator's rigid links are serially articulated. This design preserves the advantages associated with cable-driven parallel mechanisms, and introduces the advantages in having a serial kinematic structure. The kinematic and kinetic analysis is presented, with focus on the different types of cable routings. Several aspects of the manipulator design and assumptions are also discussed. The solving of inverse dynamics and wrench-closure workspace problems are important in the control and analysis of the mechanism. A detailed example for a two-link mechanism inspired by a human arm consisting of the shoulder and elbow joints is included.

1 Introduction

Cable driven parallel manipulators are parallel mechanisms where its rigid links are replaced by cables. The cables are typically attached to the end effector on one end and to the actuator situated at the stationary base platform on the other. This class of manipulators have been widely studied due to its desirable characteristics over traditional parallel mechanisms: reduced weight and inertia, simplified modelling of dynamics, ease of transportation and construction, and ease of reconfiguration.

The use of lightweight cables with negligible inertia simplifies the dynamics, modelling and control of the system. Furthermore, cable mounting points at the base platform can be relocated to result in a highly reconfigurable system. With these advantages, a range of applications exist for cable driven robots, such as manipulation of heavy payloads for manufacturing [Albus *et al.*, 1993] and cargo handling [Oh *et al.*, 2005], building construction [Bosscher *et al.*, 2007], rehabilitation [Surdilovic and Bernhardt, 2004; Mayhew *et al.*, 2005] and exoskeletons [Yang *et al.*, 2005; Agrawal *et al.*, 2009].

A unique property of cable driven mechanisms is that cables can only be actuated unilaterally through tension and not compression (*positive cable tension*). This limitation creates challenging problems in the control of the manipulator [Oh and Agrawal, 2005a] and workspace determination [Pusey *et al.*, 2004; Barrette and Gosselin, 2005; Pham *et al.*, 2009; Stump and Kumar, 2006], where techniques for serial and rigid link parallel manipulators are not applicable to cable manipulators. The direct implication of the unilateral property of actuation introduced by the use of cables is that an n degree-of-freedom (DOF) manipulator requires at least $n+1$ cables to be completely restrained. This means that a manipulator with $(m < n+1)$ and $(m > n+1)$ cables are *incompletely restrained* and *redundantly restrained*, respectively [Ming and Higuchi, 1994]. Another drawback inherent to cable-driven parallel mechanisms is the restriction in workspace due to cable interference [Williams II and Gallina, 2002], which also occurs in rigid-link parallel mechanisms.

In this paper, different aspects of the design for a 4-DOF cable-driven mechanism are explored and presented. The proposed manipulator differs from many existing cable driven parallel mechanism as it consists of multiple links connected serially as opposed to a single end-effector platform. With this design, each cable has the potential of being connected through to multiple links (*cable routing*), resulting in coupling between links during actuation. The advantages of routing cables through serial links is that it results in a more compact design with less cable interference. This design is inspired by the structure of a human arm, where unilaterally actuated muscles are compactly arranged close to the rigid links but are able to generate a large range of motion.

The multi-link structure and possibilities of multi-

ple types of cable routing complicates the definition of the Jacobian matrix compared to single link mechanisms. Different types of routing configurations have been identified, and the systematic formulation of the Jacobian matrix is presented, extending from previous formulations that only considers a single link. Two crucial aspects of the manipulator analysis are presented, the determination and evaluation of the wrench-closure workspace, and the resolution of the inverse dynamics. The resulting tension curves from the inverse dynamics are also compared a similar single link mechanism.

The workspace and inverse dynamics analysis are important in the design and control of the manipulator, and also form the necessary components required for the optimisation of the cable mounting locations for the manipulator. The ease of relocating cable mounting points allow the potential having cable arrangements that are optimised for particular tasks.

The remainder of the paper is organised as follows: the kinematics, dynamics and Jacobian matrix formulation for the proposed mechanism are formulated in Section 2. Several practical design aspects and assumptions related to the construction of the mechanism are discussed in Section 3. Section 4 presents the formulation in determining and evaluating the wrench-closure workspace, and the optimisation problem is introduced. The simulation results for the workspace determination and inverse dynamics are discussed in Section 5. Section 6 concludes the paper and presents areas of future work.

2 Kinematics and Dynamics

The design of the proposed 4-DOF manipulator is shown in Figure 1.

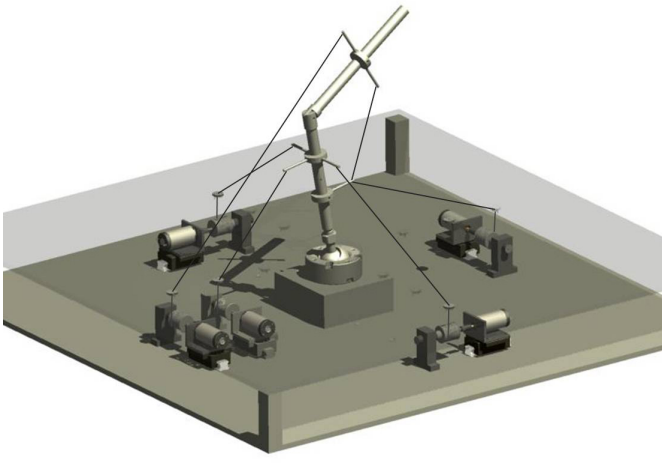

Figure 1: CAD of 4-DOF Manipulator

The manipulator consists of two links, where the first link is constrained to the base platform through a spherical joint and the two links are connected by a revolute joint. In this design, all cables are actuated from the base and can be connected to either links. Figure 2 shows the diagram of the proposed design, where A_i, B_i and C_i are the attachment points at the base, first and second links, respectively, with corresponding position vectors $\mathbf{r}_A$, $\mathbf{r}_B$ and $\mathbf{r}_C$. The vectors $\mathbf{r}_A$, $\mathbf{r}_B$ and $\mathbf{r}_C$ are constant positions in the inertial frame, $\{F_0\}$, and non-inertial frames, $\{F_1\}$ and $\{F_2\}$, respectively. Hence the attachment point for cable i can be expressed as:

$$\begin{aligned} {}^0\mathbf{r}_{A_i} &= r_{A_ix}\mathbf{i}_0 + r_{A_iy}\mathbf{j}_0 + r_{A_iz}\mathbf{k}_0 \\ {}^1\mathbf{r}_{B_i} &= r_{B_ix}\mathbf{i}_1 + r_{B_iy}\mathbf{j}_1 + r_{B_iz}\mathbf{k}_1 \\ {}^2\mathbf{r}_{C_i} &= r_{C_ix}\mathbf{i}_2 + r_{C_iy}\mathbf{j}_2 + r_{C_iz}\mathbf{k}_2 \end{aligned} \quad (1)$$

where ${}^0\mathbf{r}$,${}^1\mathbf{r}$ and ${}^2\mathbf{r}$ represents the vector $\mathbf{r}$ in $\{F_0\}, \{F_1\}$ and $\{F_2\}$, respectively.

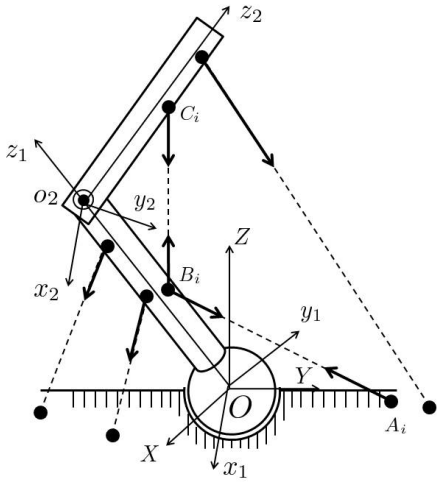

Figure 2: Model of 4-DOF Manipulator

The location of the revolute joint can be expressed by vector $\mathbf{r}_{Oo_2}$ that is constant in $\{F_1\}$. The set of generalised coordinates of the manipulator can be represented by $\mathbf{q} = \begin{bmatrix} \alpha & \beta & \gamma & \theta \end{bmatrix}^T$, where α, β and γ represents the xyz-Euler angles of the first link, and θ is the relative angle between link 1 and link 2.

2.1 Kinematics

The lengths of the m-cables present in the manipulator can be denoted as $\mathbf{l} = \begin{bmatrix} l_1 & l_2 & \dots & l_m \end{bmatrix}^T$, where l_i is the length of cable i. The cable vector is dependent on the type of cable connection and the kinematic relationship can be classified into four categories:

1. **Type 1** : Cable connecting from base to link 1

$$\mathbf{l}_i = \mathbf{r}_{Oo_1} + \mathbf{r}_{B_i} - \mathbf{r}_{A_i}$$

2. **Type 2** : Cable connecting from base to link 2

$$\mathbf{l}_i = \mathbf{r}_{Oo_2} + \mathbf{r}_{C_i} - \mathbf{r}_{A_i}$$

3. **Type 3** : Cable connecting from link 1 to link 2

$$\mathbf{l}_i = \mathbf{r}_{Oo_2} + \mathbf{r}_{C_i} - \mathbf{r}_{B_i}$$

4. **Type 4** : Cable connecting from base through link 1 to link 2

$$\begin{aligned} \mathbf{l}_{i1} &= \mathbf{r}_{Oo_1} + \mathbf{r}_{B_i} - \mathbf{r}_{A_i} \\ \mathbf{l}_{i2} &= \mathbf{r}_{Oo_2} + \mathbf{r}_{C_i} - \mathbf{r}_{B_i} \end{aligned}$$

where $\mathbf{l_{i1}}$ and $\mathbf{l_{i2}}$ represent the two segments the cable vector

The Jacobian matrix for the system can be denoted by the differential relationship:

$$\dot{\mathbf{l}} = J\dot{\mathbf{q}} \tag{2}$$

The derivative of the cable length for cable i has the following relationship:

$$\dot{l}_i = \hat{\mathbf{l}}_i \cdot \dot{\mathbf{l}}_i \tag{3}$$

Applying the relationship from (3) to cable connection **type 1**:

$$\begin{aligned} \dot{l}_i &= \hat{\mathbf{l}}_i \cdot (\dot{\mathbf{r}}_{Oo_1} + \dot{\mathbf{r}}_{B_i} - \dot{\mathbf{r}}_{A_i}) \\ &= {}^1\hat{\mathbf{l}}_i \cdot ({}^1\dot{\mathbf{r}}_{Oo_1} + {}^1\dot{\mathbf{r}}_{B_i}) \\ &= {}^1\hat{\mathbf{l}}_i \cdot ({}^1\dot{\mathbf{r}}_{Oo_1} + {}^1\boldsymbol{\omega}_1 \times {}^1\mathbf{r}_{B_i}) \\ &= {}^1\hat{\mathbf{l}}_i \cdot {}^1\dot{\mathbf{r}}_{Oo_1} + ({}^1\mathbf{r}_{B_i} \times {}^1\hat{\mathbf{l}}_i) \cdot {}^1\boldsymbol{\omega}_1 \\ &= \begin{bmatrix} ({}^1\hat{\mathbf{l}}_i)^T & ({}^1\mathbf{r}_{B_i} \times {}^1\hat{\mathbf{l}}_i)^T & 0 & 0 \end{bmatrix} \begin{bmatrix} {}^1\dot{\mathbf{r}}_{Oo_1} \\ {}^1\boldsymbol{\omega}_1 \\ {}^2\dot{\mathbf{r}}_{Oo_2} \\ {}^2\boldsymbol{\omega}_2 \end{bmatrix} \end{aligned}$$

Hence:

$$\dot{l}_i = \begin{bmatrix} A_{i11} & A_{i12} & A_{i13} & A_{i14} \end{bmatrix} \begin{bmatrix} {}^1\dot{\mathbf{r}}_{Oo_1} \\ {}^1\boldsymbol{\omega}_1 \\ {}^2\dot{\mathbf{r}}_{Oo_2} \\ {}^2\boldsymbol{\omega}_2 \end{bmatrix}$$

$$\begin{aligned} A_{i11} &= ({}^1\hat{\mathbf{l}}_i)^T \\ A_{i12} &= ({}^1\mathbf{r}_{B_i} \times {}^1\hat{\mathbf{l}}_i)^T \\ A_{i13} &= 0 \\ A_{i14} &= 0 \end{aligned}$$

Repeating this for the remaining connection types, the following relationships are obtained:

1. **Type 2** :

$$\begin{aligned} \dot{l}_i &= \begin{bmatrix} 0 & 0 & ({}^2\hat{\mathbf{l}}_i)^T & ({}^2\mathbf{r}_{C_i} \times {}^2\hat{\mathbf{l}}_i)^T \end{bmatrix} \begin{bmatrix} {}^1\dot{\mathbf{r}}_{Oo_1} \\ {}^1\boldsymbol{\omega}_1 \\ {}^2\dot{\mathbf{r}}_{Oo_2} \\ {}^2\boldsymbol{\omega}_2 \end{bmatrix} \\ &= \begin{bmatrix} A_{i21} & A_{i22} & A_{i23} & A_{i24} \end{bmatrix} \begin{bmatrix} {}^1\dot{\mathbf{r}}_{Oo_1} \\ {}^1\boldsymbol{\omega}_1 \\ {}^2\dot{\mathbf{r}}_{Oo_2} \\ {}^2\boldsymbol{\omega}_2 \end{bmatrix} \end{aligned}$$

$$\begin{aligned} A_{i11} &= 0 \\ A_{i12} &= 0 \\ A_{i13} &= ({}^2\hat{\mathbf{l}}_i)^T \\ A_{i14} &= ({}^2\mathbf{r}_{C_i} \times {}^2\hat{\mathbf{l}}_i)^T \end{aligned}$$

2. **Type 3** :

$$\dot{l}_i = \begin{bmatrix} A_{i31} & A_{i32} & A_{i33} & A_{i34} \end{bmatrix} \begin{bmatrix} {}^1\dot{\mathbf{r}}_{Oo_1} \\ {}^1\boldsymbol{\omega}_1 \\ {}^2\dot{\mathbf{r}}_{Oo_2} \\ {}^2\boldsymbol{\omega}_2 \end{bmatrix}$$

$$\begin{aligned} A_{i31} &= -({}^1\hat{\mathbf{l}}_i)^T \\ A_{i32} &= -({}^1\mathbf{r}_{B_i} \times {}^1\hat{\mathbf{l}}_i)^T \\ A_{i33} &= ({}^2\hat{\mathbf{l}}_i)^T \\ A_{i34} &= ({}^2\mathbf{r}_{C_i} \times {}^2\hat{\mathbf{l}}_i)^T \end{aligned}$$

3. **Type 4** :

$$\dot{l}_i = \begin{bmatrix} A_{i41} & A_{i42} & A_{i43} & A_{i44} \end{bmatrix} \begin{bmatrix} {}^1\dot{\mathbf{r}}_{Oo_1} \\ {}^1\boldsymbol{\omega}_1 \\ {}^2\dot{\mathbf{r}}_{Oo_2} \\ {}^2\boldsymbol{\omega}_2 \end{bmatrix}$$

$$\begin{aligned} A_{i41} &= ({}^1\hat{\mathbf{l}}_{i1} - {}^1\hat{\mathbf{l}}_{i2}) \\ A_{i42} &= ({}^1\mathbf{r}_{B_i} \times ({}^1\hat{\mathbf{l}}_{i1} - {}^1\hat{\mathbf{l}}_{i2}))^T \\ A_{i43} &= ({}^2\hat{\mathbf{l}}_{i2})^T \\ A_{i44} &= ({}^2\mathbf{r}_{C_i} \times {}^2\hat{\mathbf{l}}_{i2})^T \end{aligned}$$

The resulting kinematic relationship can be represented in the form:

$$\dot{\mathbf{l}} = J_x\dot{\mathbf{x}} \tag{4}$$

where:

$$\begin{bmatrix} \vdots \\ \dot{l}_a \\ \vdots \\ \dot{l}_b \\ \vdots \\ \dot{l}_c \\ \vdots \\ \dot{l}_d \end{bmatrix} = \begin{bmatrix} \vdots & & & \vdots \\ A_{a11} & A_{a12} & A_{a13} & A_{a14} \\ \vdots & & & \vdots \\ A_{b21} & A_{b22} & A_{b23} & A_{b24} \\ \vdots & & & \vdots \\ A_{c31} & A_{c32} & A_{c33} & A_{c34} \\ \vdots & & & \vdots \\ A_{d41} & A_{d42} & A_{d43} & A_{d44} \end{bmatrix} \begin{bmatrix} {}^1\dot{\mathbf{r}}_{Oo_1} \\ {}^1\boldsymbol{\omega}_1 \\ {}^2\dot{\mathbf{r}}_{Oo_2} \\ {}^2\boldsymbol{\omega}_2 \end{bmatrix}$$

where cables a, b, c, and d are classified as cable connection types 1, 2, 3, and 4, respectively. Finally, the relationship between $\dot{\mathbf{x}}$ and the time derivative of the task space, $\dot{\mathbf{q}}$, can be expressed as:

$$\dot{\mathbf{x}} = W\dot{\mathbf{q}} \tag{5}$$

where W is an $n \times 12$ matrix [Sui and Zhao, 2004]. Hence the kinematic relationship and jacobian from (2) can be determined by combining (4) and (5):

$$J = J_x W \tag{6}$$

2.2 Dynamics

The general form equations of motion for the 4-DOF m-cable system can be defined as:

$$M(\mathbf{q})\ddot{\mathbf{q}} + C(\mathbf{q}, \dot{\mathbf{q}}) + G(\mathbf{q}) = -J^T(\mathbf{q})\mathbf{t}, \tag{7}$$

where $\mathbf{q}$ is the manipulator pose, $M(\mathbf{q})$, $C(\mathbf{q}, \dot{\mathbf{q}})$, and $G(\mathbf{q})$ are the mass inertia matrix, the centrifugal and Coriolis components, and the gravitational components of the system dynamics, respectively. The cable wrench vector is denoted by $-J^T\mathbf{t}$, where $-J^T(\mathbf{q}) \in \mathbb{R}^{4\times m}$ represents the direction of the forces and moments generated by the actuated cables, and $\mathbf{t} = \begin{bmatrix} t_1 & t_2 & \dots & t_m \end{bmatrix}^{\mathbf{T}}$ is the cable force vector containing the magnitudes of the tension for individual cables, where t_i is the tension in cable i. In general case, each cable have an operational range of tension

$$0 < t_{i,min} \leq t_i \leq t_{i,max}, \tag{8}$$

where $t_{i,min}$ ensures positive cable tension and prevents any slack in the cable, while $t_{i,max}$ provides an upper bound on the allowable actuation.

Inverse Dynamics Problem

For a given manipulator trajectory, $\mathbf{q}(t)$, the dynamics equation from (7) can be expressed as a linear system of equations:

$$-J^T\mathbf{t} = \mathbf{b}, \tag{9}$$

where $\mathbf{b} = \mathbf{M}(\mathbf{q})\ddot{\mathbf{q}} + \mathbf{C}(\mathbf{q}, \dot{\mathbf{q}}) + \mathbf{G}(\mathbf{q})$. The inverse dynamics problem requires determining the set of cable tensions, $\mathbf{t}$, subject to the constraints on tension (8) while satisfying (9). For completely and redundantly restrained cable systems [Ming and Higuchi, 1994], there exists an infinite number of solutions to the inverse dynamics problem. This issue can be resolved by introducing an objective function based on cable tensions [Oh and Agrawal, 2005b; Hassan and Khajepour, 2008; Borgstrom *et al.*, 2009]. The types of optimisation problem that results depend on the complexity of the objective functions. One common objective can be expressed as:

$$\min \mathbf{t}^T H \mathbf{t} \tag{10}$$

where H is a positive definite matrix. A quadratic programming problem results with the quadratic objective function (10), and linear constraints (8) and (9).

Evaluation of Trajectory Tension

Assuming the goal of minimisation of energy, or tension required, by the system to perform a particular trajectory, it is apparent that the objective function employed in the inverse dynamic optimisation problem (10) should be utilised. Hence to perform a particular trajectory $\mathbf{x}(\mathbf{t})$ from time $t = 0$ to $t = t_{total}$ requires tension, $\mathbf{t}(t)$, the overall cost can be defined as:

$$Q = \int_0^{t_{total}} \mathbf{t}^T H \mathbf{t} \; dt \tag{11}$$

This Q function is important in the optimisation of cable routing and arrangements for the execution of a particular or a set of desired trajectories.

3 Mechanism Design

The CAD model of the proposed manipulator is shown in Figure 1. In the kinematic and dynamic models presented in Sections 2.1 and 2.2, several aspects have been assumed to be ideal to simplify the dynamics of the system.

Firstly, the cable is assumed to be massless and rigid. This simplifies the motor control required to ensure the desired set of tension, $\mathbf{t}$, is generated. The selection criteria for the cables include material density, the Young's modulus, flexure, and cable diameter. Selection of higher Young's modulus result in increased rigidity along the length of the cable. Cables with a smaller diameter result in lower mass of cables, but would be more flexible and less rigid. The appropriate choice of cable would depend on the performance requirements of the manipulator.

Another assumption is that cable attachment locations are fixed regardless of the kinematic posture of the manipulator. In practice, this is difficult to realise, as cables need to go through a feeding mechanism at that point, such as a pulley, with a non-zero radius, creating dependence of the cable mounting position on the kinematic posture. In this design, the cable is actuated by the motor through the cable spool, and passes through a thin hole then is attached to the end effector. The thin hole at the base acts as the fixed attachment point at the base platform, $\mathbf{r}_A$. Despite having a fixed attachment at the base, cable wrapping as well as the shift in the location where the cable comes in contact with the spool while winding and unwinding is still an issue for the purpose of forward kinematics and control.

The proposed solution to this problem is to design the motor and spool mechanism such that as the cable winds

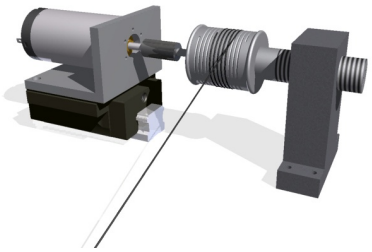

Figure 3: Cable Spool Design

and unwinds, the spool also moves axially in an appropriate manner. The proposed design is shown in Figure 3, where the motor is mounted onto a linear rail with the spool mounted on the motor shaft. The other end of the shaft is constrained by a support block through a threaded screw and nut arrangement forming a helical joint. The threaded screw constrains the linear motion of the spool depending on the rotation of the spool/shaft such that the distance between the point of cable leaving the spool to the hole at the base is fixed. The relationship between the cable length.

4 Wrench-Closure Workspace Analysis

Knowledge of the end effector's usable workspace is essential for several purposes, such as the trajectory planning [Valero *et al.*, 2006] and the selection and design of manipulator configurations depending on the workspace requirements [Perreault and Gosselin, 2008]. The *configuration* of a cable driven manipulator refers to the location of cable attachments at the base platform and the end effector.

The *wrench-closure workspace* (WCW) is defined as the set of poses in which the manipulator can sustain any arbitrary external wrench when no upper bounds are placed on the cable tensions. This is an idealised assumption on the manipulator as cables would realistically satisfy the constraints from (8). Despite this limitation, the WCW is a useful workspace analysis technique to study the capability of the manipulator assuming that the motion dynamics can be achieved within the cable maximum tension.

The *wrench-closure condition* (WCC) for a particular pose is satisfied if a set of positive cable tensions can be determined for any arbitrary external wrench, velocity or acceleration of the manipulator without any upper bound to cable tension. Combining the terms representing the dynamics of the system, the equation of motion (7) can be expressed as:

$$\mathbf{w} = J^T\mathbf{t} \tag{12}$$

where $\mathbf{w} = -[M(\mathbf{q})\ddot{\mathbf{q}} + C(\mathbf{q},\dot{\mathbf{q}}) + G(\mathbf{q}) + F_{ext}(\mathbf{q})]$. Hence for an n-DOF m-cable system, the WCC can be described as:

$$\forall \mathbf{w} \in \mathbb{R}^n, \exists \mathbf{t} > \mathbf{0} : J^T\mathbf{t} = \mathbf{w} \tag{13}$$

where $\mathbf{t} > 0$ means that all cable tensions are positive. The geometrical interpretation of (13) is that the WCC is satisfied if the columns of J^T positively span $\mathbb{R}^n$ for full rank J^T. An equivalent definition of the WCC is the existence of some positive cable tension vector within the nullspace of J^T [Gouttefarde and Gosselin, 2006].

$$\begin{aligned} &rank(J^T) = n \\ &\exists \mathbf{t} \in ker(J^T) : \mathbf{t} > 0 \end{aligned} \tag{14}$$

Another interpretation of (13) is that the WCC can be described by performing row reduction on the linear system. Since J^T is of full rank, and considering a completely restrained system, $m = n + 1$, the $n \times (n + 1)$ transpose of the Jacobian matrix can be expressed in reduced row echelon form:

$$J^T \rightarrow \left[\ I_n \mid \mathbf{v}(\mathbf{q})\ \right] \tag{15}$$

where $I_n \in \mathbb{R}^{n\times n}$ is an identity matrix and $\mathbf{v} \in \mathbb{R}^n$ is a function of the pose variables. Applying the row reduction as in (15) on the WCC in (13):

$$\left[\ I_n \mid \mathbf{v}(\mathbf{q})\ \right]\mathbf{t} = \mathbf{w}', \mathbf{t} > \mathbf{0} \tag{16}$$

where $\mathbf{w}'$ is the wrench vector after row reduction. The interpretation of (16) is that if all components of $\mathbf{v}$ are negative, $\mathbf{v} < \mathbf{0}$, WCC is be satisfied. This can be shown by observing the set of equations from (16):

$$t_j + v_j(\mathbf{q})t_m = w'_j, \forall j \in 1, \ldots, n \tag{17}$$

where j refers to the j^{th} row of (16). Given that $t_m \in (0, \infty)$, if $v_j(\mathbf{q}) < 0$, then $v_j t_m \in (-\infty, 0)$ and hence $w'_j \in (-\infty, \infty)$. The result of this is $\mathbf{w} \in \mathbb{R}^n$, satisfying the WCC from (13). The WCW for the manipulator is defined as the set of poses in which the WCC is satisfied. This can be defined as:

$$\{\mathbf{q} : \forall \mathbf{w} \in \mathbb{R}^n, \exists \mathbf{t} > 0, J^T(\mathbf{q})\mathbf{t} = \mathbf{w}\} \tag{18}$$

An alternative definition of WCC using (16) can also be used to define the WCW:

$$\left\{\mathbf{q} : \mathbf{v}(\mathbf{q}) < \mathbf{0}, J^T \rightarrow \left[\ I_n \mid \mathbf{v}(\mathbf{q})\ \right]\right\} \tag{19}$$

Hence the resulting workspace can be considered as the intersection of a set of multivariate inequalities. Knowledge of the algebraic form of $\mathbf{v}(\mathbf{q})$, derived in the following section, is required to analytically determine the workspace region. It can also be shown that the WCW boundary is comprised of sections of the curves $\mathbf{v}(\mathbf{q}) = \mathbf{0}$.

By selecting one of the pose variables, for example, α, setting all other pose variables constant, allows the determination of the WCW from (19) can be expressed as:

$$\{\alpha : v_j(\alpha) < 0, \forall v_j(\alpha) \in \mathbf{v}(\mathbf{q})\} \tag{20}$$

where j represents the rows of the vector $\mathbf{v}$. Hence it is possible to determine, either analytically or numerically a set of lower and upper bounds for α that represent the workspace:

$$\{\alpha : v_j(\alpha) < 0, \forall j, \alpha \in (\alpha_{lower}, \alpha_{upper})\} \tag{21}$$

Running iterations through the other pose variables (hence these pose variables are constant within the iteration) allows us to obtain the picture of the WCW over the workspace of interest.

4.1 Workspace Evaluation

The determination of WCW and expression with respect to a single variable in the form of (21) allows efficient evaluation of the workspace based on a desired objective function. This allows direct comparison between different configurations in an autonomous manner. Introducing a function f that evaluates the quality of a desired pose, $\mathbf{q} = (\alpha, \beta, \gamma, \theta)$, the total quality of the workspace can be defined as:

$$Q = \int_\theta \int_\gamma \int_\beta \int_\alpha f(\mathbf{q})\ d\alpha\ d\beta\ d\gamma d\theta,\ \forall \mathbf{q} \in W \tag{22}$$

where W represents the WCW of the manipulator. The function f can be constructed depending on the desired objective to be measured. For example, if the volume is to be measured, the following function can be used:

$$f(\mathbf{q}) = 1 \tag{23}$$

In this evaluation, each point of the workspace volume is weighted equally. In some scenarios, it may be more appropriate to weight certain regions. The quality function in (24) weights poses that are closer in Euclidian distance to the desired pose $(\alpha_s, \beta_s, \gamma_s, \theta_s)$.

$$f(\mathbf{q}) = \frac{1}{1 + D^2} \tag{24}$$

where:

$$D^2 = (\alpha - \alpha_s)^2 + (\beta - \beta_s)^2 + (\gamma - \gamma_s)^2 + (\theta - \theta_s)^2$$

It can be then shown that the quality Q can be very efficiently evaluated given that the integral function of $f(\alpha, \beta, \gamma, \theta)$, denoted by $F(\alpha, \beta, \gamma, \theta)$, can be determined analytically with respect to a single variable.

For example, assuming that the workspace is expressed in the form of (21) with respect to α, the quality can be described as:

$$Q = \sum_\theta \sum_\gamma \sum_\beta \sum_k \int_{\alpha_{u_l}}^{\alpha_{u_k}} f(\mathbf{q})\ d\alpha,\ \forall \mathbf{q} \in W \tag{25}$$

where k represents the number of (α_l, α_u) intervals at the β and γ value. Substituting the integral function, $F(\alpha, \beta, \gamma)$, to (25), the quality could be further simplified to form:

$$Q = \sum_\theta \sum_\gamma \sum_\beta \sum_k F(\alpha_{u_k}) - F(\alpha_{u_l}),\ \forall \mathbf{q} \in W \tag{26}$$

The total quality from (26) provides an efficient way to evaluate the quality of a workspace determined using the proposed representation of the WCW.

4.2 Optimisation Problem

The optimisation problem of cable configuration involves the determination of cable attachment locations subject to design constraints to achieve a desired goal. This can be formulated as:

$$\mathbf{r}_A^*, \mathbf{r}_B^*, \mathbf{r}_C^* = \underset{\mathbf{r}_A, \mathbf{r}_B, \mathbf{r}_C}{\arg\max}\, Q(\mathbf{r}_A, \mathbf{r}_B, \mathbf{r}_C), \tag{27}$$

subject to:

$$\mathbf{r}_A \in \mathcal{A}, \mathbf{r}_B \in \mathcal{B}, \mathbf{r}_C \in \mathcal{C} \tag{28}$$

where $\mathbf{r}_A^*$, $\mathbf{r}_B^*$, and $\mathbf{r}_C^*$ are the optimal cable attachment locations at the base, link 1 and link 2, respectively. The sets $\mathcal{A}$, $\mathcal{B}$ and $\mathcal{C}$ used for the constraint of the problem represents the limitation in the possible attachment locations, for example, $\mathcal{B}$ would represent the surface of link 1. In this optimisation problem, the achieved goal would be a cable configuration that maximises a certain desired quality, for example, volume.

For the case of inverse dynamics, the cost function from (11) could be utilised with the goal of minmising the overall energy, and hence the problem becomes:

$$\mathbf{r}_A^*, \mathbf{r}_B^*, \mathbf{r}_C^* = \underset{\mathbf{r}_A, \mathbf{r}_B, \mathbf{r}_C}{\arg\min}\, Q(\mathbf{r}_A, \mathbf{r}_B, \mathbf{r}_C), \tag{29}$$

subject to the same constraints. Optimisation with these goals is very specific to a specific task, and is certainly feasible in this class of highly reconfigurable manipulators.

5 Simulation and Results

5.1 Simulation Setup

For the analysis of dynamics and WCW of the proposed mechanism as presented in Sections 2 and 4, respectively, two different cable arrangements for the proposed mechanism is considered. In configuration A, as shown in Figure 4, the second link is assumed to be massless, simplifying the system to a single link 3-DOF manipulator.

For a single link 3-DOF manipulator, $m \geq 4$ cables are required to completely or redundantly restrain the system. In configuration A, a completely restrained system of $m = 4$ have been considered, and the cables are arranged symmetrically around the manipulator as shown

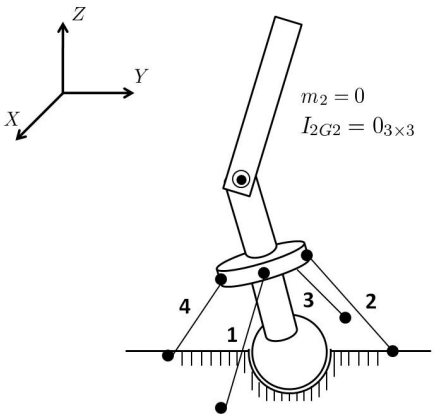

Figure 4: Diagram of Cable Configuration A

in Figure 4. The analysis of this configuration is important in the verification and understanding for the two-link system.

Figure 5 shows the cable arrangement of configuration B, a two-link 4-DOF redundantly restrained manipulator actuated by $m = 6$ cables. Configuration B has the same cable attachments for cables 1 to 4 as shown in Figure 4, and adds two additional type 4 cables (refer to Section 2.1), cables 5 and 6. Cables 5 and 6 are responsible for the actuation of link 2, and it is important to note that its actuation will also affecting the motion of link 1 due to the revolute joint and also cable routing through the link.

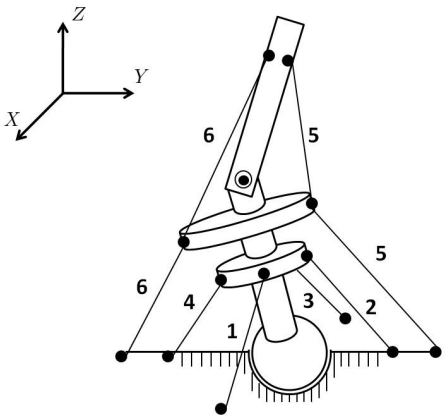

Figure 5: Diagram of Cable Configuration B

5.2 WCW Determination

The WCW analysis and evaluation presented in Section 4 is simulated for configuration A. From the Jacobian matrix and dynamics model derived in (6) and (7), it is apparent that the definition of the WCW in (21) is identical for the single link 3-DOF and two link 4-DOF manipulators, differing only in the dimension of the Jacobian matrix. Hence for the purpose of visualisation, the WCW of only the 3-DOF system is shown in this section.

For the system in configuration A, $\mathbf{q} = \begin{bmatrix} \alpha & \beta & \gamma \end{bmatrix}^T$, and the resulting WCW is shown in Figures 6, 7 and 8. The α-β, Euler angles in x and y, cross sections for various γ values are shown to represent the 3-D workspace of the pose variables.

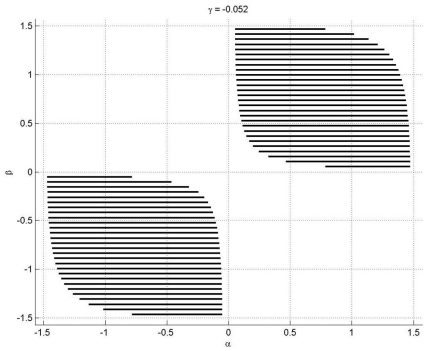

Figure 6: WCW α-β cross-sections at $\gamma = -\frac{\pi}{60}$

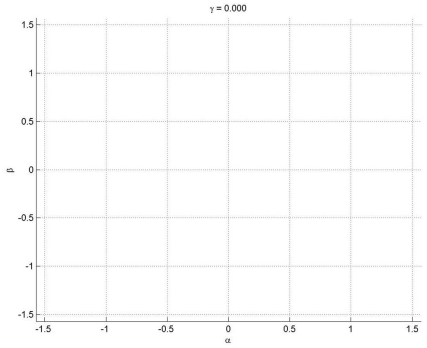

Figure 7: WCW α-β cross-sections at $\gamma = 0$

Due to the symmetry of the cable arrangements, it can be observed that the workspace possesses symmetry about the point $\alpha = \beta = \gamma = 0$. The empty plane at $\gamma = 0$ in Figure 6 exists due to singularities in the system, separating the regions observed from Figures 7 and 8. In essence, the manipulator is singular at $\gamma = 0$. Disconnected regions in the workspace are not desired as the manipulator is not able to travel from poses in one region to another, rendering disconnected regions unusable. From the WCW, the manipulator's operational ability of the manipulator can be determined.

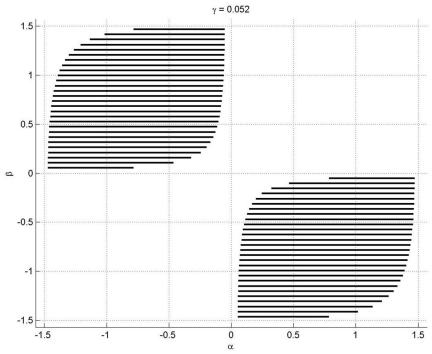

Figure 8: WCW α-β cross-sections at $\gamma = \frac{\pi}{60}$

5.3 Inverse Dynamics

The inverse dynamics for configurations A and B are simulated for a simple test trajectory. The selected trajectory is rotational motion about the X axis shown in Figures 4 and 5, from an angle of $\alpha = \frac{\pi}{4}$ to $\alpha = -\frac{\pi}{4}$. The other poses are set to be $\beta = \gamma = \theta = 0$ for the whole trajectory.

Figure 9 shows the resulting tension curves for the 4 actuating cables. For the first half of the trajectory, cable 2 is required to exert tension to balance the weight of the manipulatory. At $t = 0.25s$, the trajectory is at dead centre position, $\alpha = \beta = \gamma = 0$, and after this point, cable 4 is actuates to control the manipulator. It can be observed that the maximum tension for the trajectory is approximately $35N$. Cables 2 and 3 exert no tension as motion of the end effector is purely in the Y-Z plane.

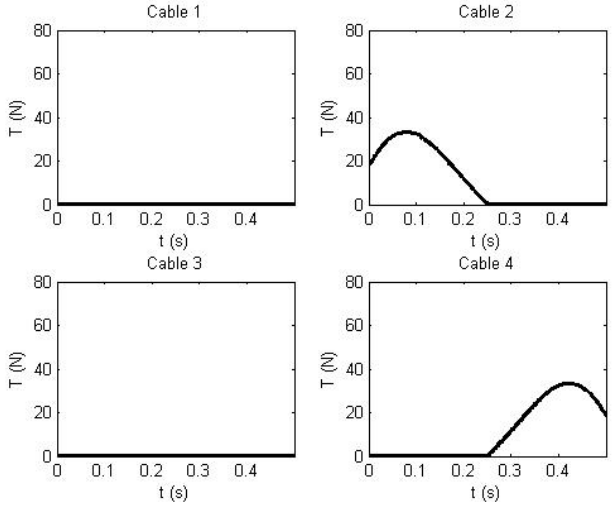

Figure 9: Inverse Dynamics for Configuration A

For configuration B, the identical trajectory is simulated and the resulting tension curves are shown in Figure 10. Likewise to configuration A, cables 1 and 3 do not exert any tension. In configuration B, cables 5 and 6 are the only ones available to control the position of the upper link. For the first half of the trajectory, tension in cable 5 is required to balance the weight of the upper link, with a maximum tension of approximately $55N$. This force is also transmitted through the first link, and can be observed to be larger than the tension required to control the motion of the link as demonstrated in configuration A. As a result, the actuation of cable 4 is necessary, of a maximum of approximately $20N$, to counterbalance the actuation of cable 5 such that the desired motion for link 1 is satisfied.

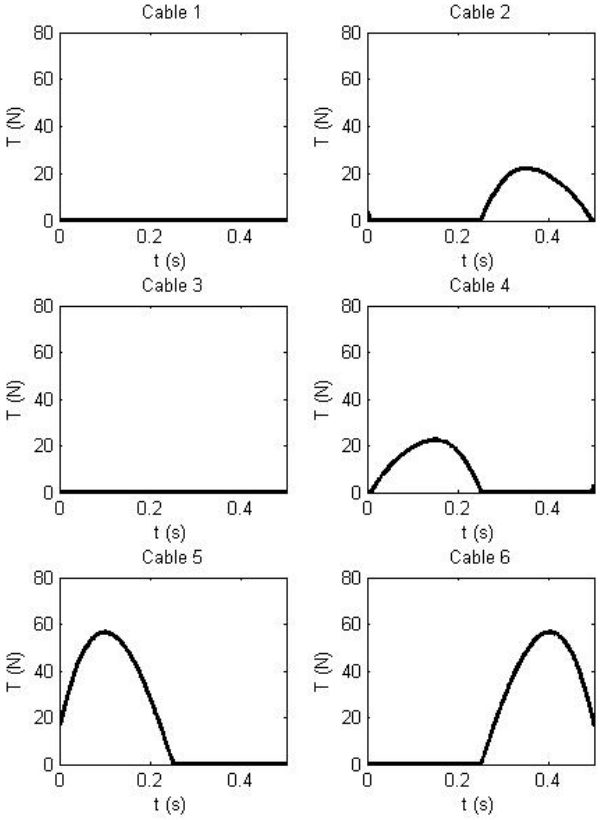

Figure 10: Inverse Dynamics for Configuration B

The presented test cases verifies the Jacobian matrix and dynamics model for the proposed two-link serial mechanism. The ability to construct a generalised Jacobian matrix while considering cable routing combinations is important to allow flexibility in the design of this type multi-link cable mechanisms.

6 Conclusion and Future Work

The design and analysis of a multi-link serially articulated manipulator actuated by cables in parallel was presented. The kinematics and dynamics modelling of single link cable driven manipulators was extended to consider cable routing through multiple links. Two types of analysis, the wrench-closure workspace and inverse dynamics were presented and simulation results show the validity of the proposed model. The ability to have cable routing results in a more compact design while preserving the advantages of cable driven mechanisms. Future work will focus on the optimisation problem of cable arrangements and verification of the model on the constructed manipulator.

References

[Agrawal *et al.*, 2009] S. K. Agrawal, V. N. Dubey, J. J. Gangloff, Jr., E. Brackbill, Y. Mao, and V. Sangwan. Design and optimization of a cable driven upper arm exoskeleton. *J. Med. Dev.*, 3:031004, 2009.

[Albus *et al.*, 1993] J. S. Albus, R. V. Bostelman, and N. Dagalakis. The NIST robocrane. *J. Rob. Sys.*, 10(5):709–724, 1993.

[Barrette and Gosselin, 2005] G. Barrette and C. M. Gosselin. Determination of the dynamic workspace of cable-driven planar parallel mechanisms. *J. Mech. Des.*, 127:242–248, 2005.

[Borgstrom *et al.*, 2009] P. H. Borgstrom, B. L. Jordan, G. S. Sukhatme, M. A. Batalin, and W. J. Kaiser. Rapid computation of optimally safe tension distributions for parallel cable-driven robots. *IEEE Trans. Rob.*, 25(6):1271–1281, 2009.

[Bosscher *et al.*, 2007] P. Bosscher, R. L. Williams II, L. S. Bryson, and D. Castro-Lacouture. Cable-suspended robotic contour crafting system. *Autom. Constr.*, 17:45–55, 2007.

[Gouttefarde and Gosselin, 2006] M. Gouttefarde and C. M. Gosselin. Analysis of the wrench-closure workspace of planar parallel cable-driven mechanisms. *IEEE Trans. Rob.*, 22(3):434–445, 2006.

[Hassan and Khajepour, 2008] M. Hassan and A. Khajepour. Optimization of actuator forces in cable-based parallel manipulators using convex analysis. *IEEE Trans. Rob.*, 24(3):736–740, 2008.

[Mayhew *et al.*, 2005] D. Mayhew, B. Bachrach, W. Z. Rymer, and R. F. Beer. Development of the MACARM - a novel cable robot for upper limb neurorehabilitation. In *Proc. IEEE Int. Conf. Rehab. Rob.*, pages 299–302, 2005.

[Ming and Higuchi, 1994] A. Ming and T. Higuchi. Study on multiple degrees-of-freedom positioning mechanism using wires (part 1) - concept, design and control. *Int. J. Japan Social Eng.*, 28(2):131–138, 1994.

[Oh and Agrawal, 2005a] S.-R. Oh and S. K. Agrawal. Cable suspended planar robots with redundant cables: Controllers with positive tension. *IEEE Trans. Rob.*, 21(3):457–464, 2005.

[Oh and Agrawal, 2005b] S.-R. Oh and S. K. Agrawal. Cable suspended planar robots with redundant cables: Controllers with positive tension. *IEEE Trans. Rob.*, 21(3):457–464, 2005.

[Oh *et al.*, 2005] S.-R. Oh, K. Mankala, S. K. Agrawal, and J. S. Albus. A dual-stage planar cable robot: Dynamic modelling and design of a robust controller with positive inputs. *J. Mech. Des.*, 127:612–620, 2005.

[Perreault and Gosselin, 2008] S. Perreault and C. M. Gosselin. Cable-driven parallel mechanisms: Application to a locomotion interface. *J. Mech. Des.*, 130:102301, 2008.

[Pham *et al.*, 2009] C. B. Pham, S. H. Yeo, G. Yang, and I-M. Chen. Workspace analysis of fully restrained cable-driven manipulators. *Rob. and Auton. Sys.*, 57:901–912, 2009.

[Pusey *et al.*, 2004] J. Pusey, A. Fattah, S. Agrawal, and E. Messina. Design and workspace analysis of a 6-6 cable-suspended parallel robot. *Mech. Mach. Theory*, 39:761–778, 2004.

[Stump and Kumar, 2006] E. Stump and V. Kumar. Workspaces of cable-actuated parallel manipulators. *J. Mech. Des.*, 128:159–167, 2006.

[Sui and Zhao, 2004] C. Sui and M. Zhao. Control of a 3-dof parallel wire driven stiffness-variable manipulator. pages 204–209, 2004.

[Surdilovic and Bernhardt, 2004] D. Surdilovic and R. Bernhardt. STRING-MAN: A new wire robot for gait rehabilitation. In *Proc. IEEE Int. Conf. Rob. Autom.*, pages 2031–2036, 2004.

[Valero *et al.*, 2006] F. Valero, V. Mata, and A. Besa. Trajectory planning in workspaces with obstacles taking into account the dynamic robot behaviour. *Mech. Mach. Theory*, 41:525–536, 2006.

[Williams II and Gallina, 2002] R. L. Williams II and P. Gallina. Planar cable-direct-driven robots: Design for wrench exertion. *J. Int. Rob. Sys.*, 35:203–219, 2002.

[Yang *et al.*, 2005] G. Yang, W. Lin, M. S. Kurbanhusen, C. B. Pham, and S. H. Yeo. Kinematic design of a 7-DOF cable-driven humanoid arm: a solution-in-nature approach. In *Proc. IEEE/ASME Int. Conf. Adv. Int. Mechat.*, pages 444–449, 2005.